Supporting Information for "Combining Landau-Zener Theory and Kinetic Monte Carlo Sampling for Small Polaron Mobility of Doped $BiVO_4$ from First-principles"

Feng Wu[1] and Yuan Ping[1,*]

[1] *The Department of Chemistry and Biochemistry, University of California, Santa Cruz, 95064 CA, United States*

COMPUTATIONAL DETAILS

In this work, all structural relaxations, electronic structure and climbing-image nudged-elastic-bands (CI-NEB) calculations were performed with open source plane wave code Quantum-ESPRESSO[1, 2] package. For 3% and 6% Mo-doped $BiVO_4$ and pristine $BiVO_4$ with the equivalent electron polaron concentrations we have used a 96-atom (6%) and a 192-atom (3%) supercell respectively. DFT+U calculations were performed using Perdew-Burke-Ernzerhof (PBE) [3, 4] exchange-correlation functional,with U(V)=2.7 eV, U(Cr)=2.8 eV, U(W)=2.1 eV and U(Mo)=2.3 eV according to Ref. 5, 6. We used GBRV ultrasoft pseudopotentials[7] with a wavefunction plane wave cutoff of 50Ry and a charge density plane wave cutoff of 300Ry, and 2x2x2 k-point sampling. Hybrid calculations were performed using PBE0 and dielectric dependent hybrid functionals with an exact exchange fraction $\alpha = 0.1449$ that is determined by the inverse of high-frequency dielectric constant of $BiVO_4$ $\alpha = 1/\varepsilon_\infty$, ONCV norm-conserving pseudopotentials[8, 9], a wavefunction plane wave cutoff of 70 Ry, a charge density plane wave cutoff of 280 Ry and 1x1x1 k-point mesh. Both cell size and internal geometry were fully optimized for pristine $BiVO_4$ and only the internal geometry was further optimized for doped $BiVO_4$.

Constraint DFT calculations (CDFT) were performed with a recent implementation generalized for solids[10]. Within CDFT, an additional external potential is added to the Kohn-Sham equation, and its strength is self-consistently determined to make a specific number of electrons localied on a given site. CDFT can directly yield charge densities and reorganization energies of diabatic states. The electron coupling matrix element H_{ab} is determined from overlaps of two Slater determinants constructed from Kohn-Sham wavefunctions of two diabatic states. CDFT calculations were performed in a 192-atom supercell, ONCV norm-conserving pseudopotentials, a wavefunction plane wave cutoff of 70Ry and 1x1x1 k-point mesh, with PBE, DFT+U and hybrid functionals.

Phonons at Γ-point were computed by VASP[11–14] with PAW[15, 16] and Phonopy[17] in a 96-atoms supercell using DFT+U. A kinetic energy cutoff of 400 eV and 2x2x2 k-point mesh were used in the geometry optimization and phonon calculations. The transition state geometry for phonon calculations specifically was optimized by CI-NEB followed by a dimer method by VASP and transition state search tool (VTST)[18–21].

KINETIC MONTE CARLO SIMULATION FROM HOPPING RATES TO MOBILITY

We used kinetic Monte Carlo (kMC) simulation to predict the mobility with polaron hopping transfer rates between sites in $BiVO_4$. The kMC is a statistical method of a random process on average by means of multiple simulations. The process can be described as below[22]:

1. Set up a lattice model with multiple sites represent different V atoms. A selected group of hopping between sites are considered in the simulation, for example, only first nearest neighbor hopping, or both first (1NN) and second nearest (2NN) neighbor hopping.

2. Calculate all non-equivalent hopping rates (between 1NN) k_{ab} from the method described in the main text with the Landau-Zener theory at a specific temperature T, where a, b are sites.

3. Choose an arbitrary site as the starting point, marked as a.

4. Randomly choose the next site b to hop to: The probability to hop to the neighbor b_i is $p_i = k_{ab_i} / \sum_j k_{ab_j}$. A random number r uniformed distributed on $[0, 1)$ is generated. The site b_i is chosen if $\sum_{j=1}^{i} p_j \leq r < \sum_{j=1}^{i+1} p_j$.

5. A random number r' uniformed distributed on $[0, 1)$ is generated, and the time cost Δt in this step is $\Delta t = -\ln(r') / \sum_i k_{ab_i}$

6. Repeat the above two steps, and record the squared displacement L^2 and time per S steps until sampled M times, where S and M should be sufficiently large. The total simulation time is given by $MS\langle\Delta t\rangle$.

7. Repeat step 3 to 6 for N times, and take the average of these $L^2 - t$ curve (Each consists of M points). This would give an approximately linear curve from which we can fit the diffusion coefficient D.

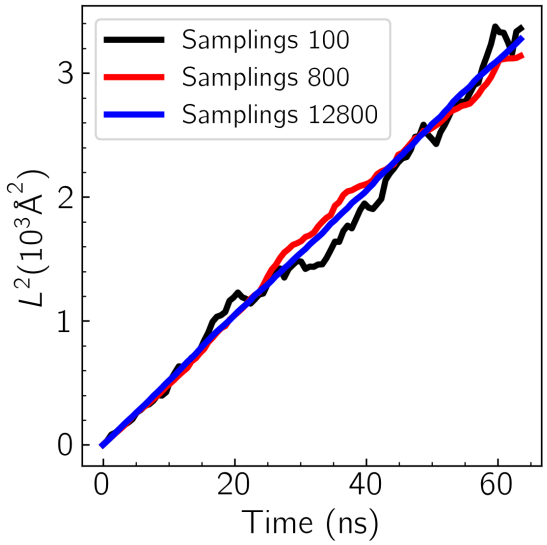

FIG. S1. The averaged square displacement over time of N=100, 800 and 12800 samplings in pristine $BiVO_4$.

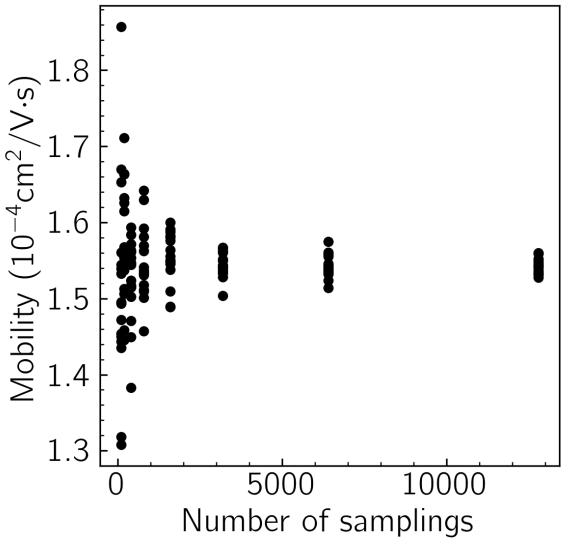

FIG. S2. The mobility v.s. number of samplings N in pristine $BiVO_4$.

8. Repeat the above steps for K times and get a set of diffusion coefficient $D_i(i = 1, 2, \cdots K)$ and following mobility $\mu_i(i = 1, 2, \cdots K)$. We can estimate the error of the mobility from this dataset as $\max(\mu_i) - \min(\mu_i)$.

Here we listed results from pristine $BiVO_4$ to illustrate the process. Fig. S1 shows the average of square displacement over time of N samplings, with $S = 10$ and $M = 100$. From Fig. S1 we can see only with enough simulations there is a good linear relationship between L^2 and t. Fig. S2 shows the mobility obtained from different number of samplings N, and for each N the simulation is repeated $K = 16$ times. It is clear that the instability decreases with increasing N. The error of mobility is shown in Fig. S3, which is smaller than 2% when $N = 12800$, which confirms the reliability of this simulation.

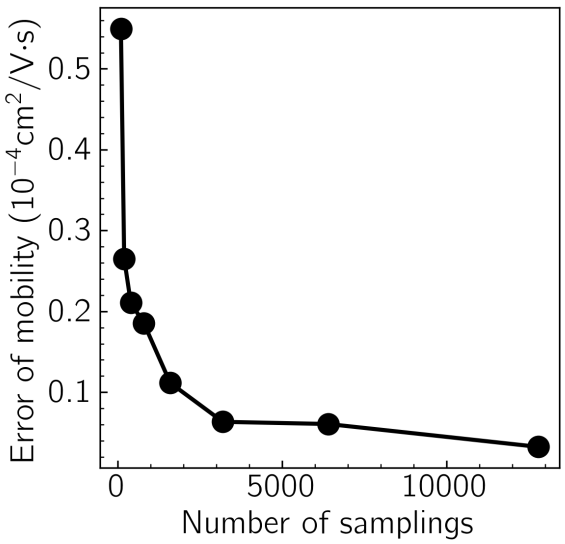

FIG. S3. The error of the mobility estimated from $\max(\{\mu_i\}) - \min(\{\mu_i\})$ with given number of samplings N in pristine $BiVO_4$.

ANISOTROPIC FIRST NEAREST NEIGHBOR HOPPING IN $BiVO_4$

Here we will demonstrate why the first nearest neighbor hopping in $BiVO_4$ is anisotropic.

In a periodic system with only one equivalent site that has 4 equivalent nearest neighbors as Fig.S4, each hopping always gives the same square displacement $L_i^2(i = x, y, z)$:

$$L_x^2 = a^2/2 \quad (1)$$
$$L_y^2 = b^2/2 \quad (2)$$
$$L_z^2 = c^2/2 \quad (3)$$

Because the diffusion coefficient along each direction follows $D_i = L_i^2/2\Delta t$, only when $a = b = c$ we have $D_x = D_y = D_z$. In $BiVO_4$, $a \approx b$ and $c/a = 1.6$, this gives the mobility a/c ratio 0.38 in the main text.

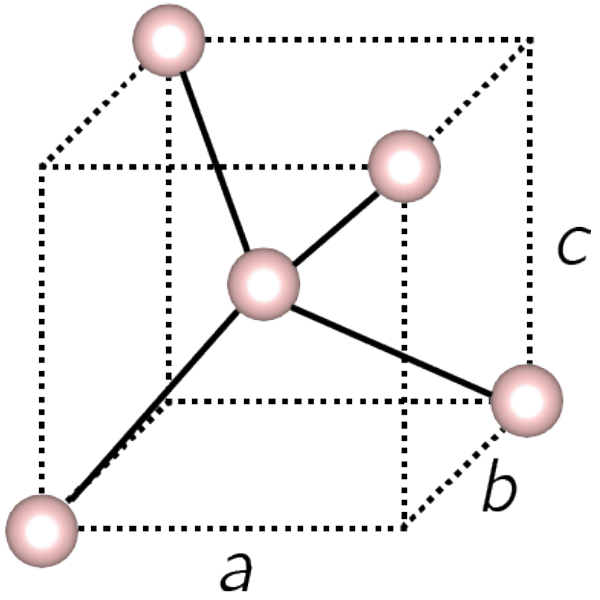

FIG. S4. A site with four equivalent nearest neighbors

EFFECTIVE FREQUENCY CALCULATION

The effective frequency in the Landau-Zener theory can be computed from partition functions:

$$\begin{aligned}\nu_{\text{eff}} &= \frac{k_B T}{h}\frac{Z_{\text{TS}}}{Z_{\text{GS}}} \\ &= \frac{k_B T}{h}\frac{\prod_i^{3N-6}\left[2\sinh\left(\frac{h\nu_i^{\text{GS}}}{2k_BT}\right)\right]}{\prod_i^{3N-7}\left[2\sinh\left(\frac{h\nu_i^{\text{TS}}}{2k_BT}\right)\right]}\end{aligned} \tag{4}$$

At the high temperature limit, $k_BT \gg h\nu_i$, we have

$$2\sinh\left(\frac{h\nu}{2k_BT}\right) \to \frac{h\nu}{k_BT} \tag{5}$$

and

$$\begin{aligned}\nu_{\text{eff}} &= \frac{k_B T}{h}\frac{\prod_i^{3N-6}\left[2\sinh\left(\frac{h\nu_i^{\text{GS}}}{2k_BT}\right)\right]}{\prod_i^{3N-7}\left[2\sinh\left(\frac{h\nu_i^{\text{TS}}}{k_BT}\right)\right]} \\ &\approx \frac{k_B T}{h}\frac{\prod_i^{3N-6}\frac{h\nu_i^{\text{GS}}}{k_BT}}{\prod_i^{3N-7}\frac{h\nu_i^{\text{TS}}}{k_BT}} \\ &= \frac{\prod_i^{3N-6} h\nu_i^{\text{GS}}}{\prod_i^{3N-7} h\nu_i^{\text{TS}}}\end{aligned} \tag{6}$$

The results are summarized in Table I. We can see the high temperature limit (Eq. 6) underestimates the effective frequency by half at 300K compared with the one obtained from partition functions (Eq. 4).

TABLE I. Effective frequencies computed with different approaches (Eq. 4 and Eq. 6) at 300K

Method	1NN $h\nu_{\text{eff}}$ (meV)	2NN $h\nu_{\text{eff}}$ (meV)
Partition function	267	285
High temperature limit	132	138

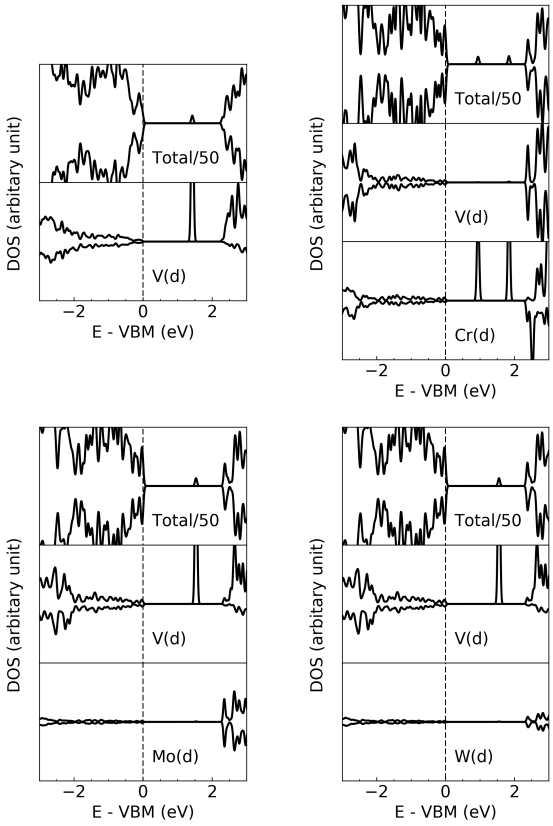

FIG. S5. Total and projected density of states of pristine (top left), Cr(top right), Mo (bottom left) and W (bottom right) doped $BiVO_4$. The total DOS is 0.02x for visualization. V(d) is the site where an electron polaron is localized at except that in the Cr-doped case. In Cr-doped $BiVO_4$ there is no polaron localized at V and the PDOS of all V are very similar, so an arbitrary one is shown here.

PROJECTED DENSITY OF STATES OF PRISTINE, CR, MO AND W DOPED $BiVO_4$

The total and projected density of states are shown in Fig. S5. The projected density of states clearly show that in the pristine, Mo-doped and W-doped $BiVO_4$, there is a filled gap state due to an excess electron localized at one V atom that corresponds to the polaron. However, in Cr-doped $BiVO_4$, there are two gap states localized at Cr instead of any V atom, which means the electron is trapped at the Cr site in this system.

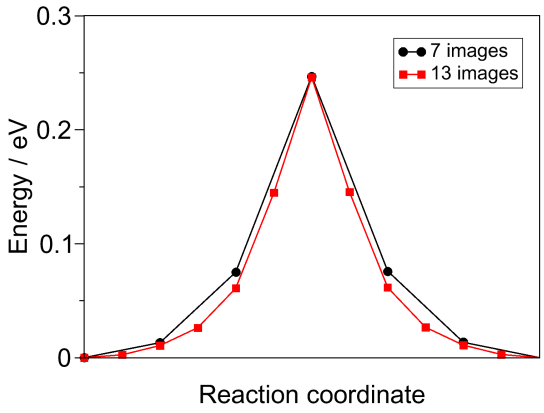

FIG. S6. Comparison of the obtained pathway of nearest neighbor polaron hopping N in pristine $BiVO_4$. from CI-NEB calculations of different number of images.

CI-NEB CALCULATIONS OF BARRIERS

All CI-NEB calculations are done with 7 images between the initial and final state. From Figure. S6 we can see the difference between the barrier in CI-NEB with 7 images and that with 13 images is smaller than 3meV.

The local structures of two VO_4 tetrahedra where the polaron hopping happens are shown in Figure. S7. The V-O bond lnegths in two VO_4 are the same at transition state and have significant difference when the polaron is localized on one of them.

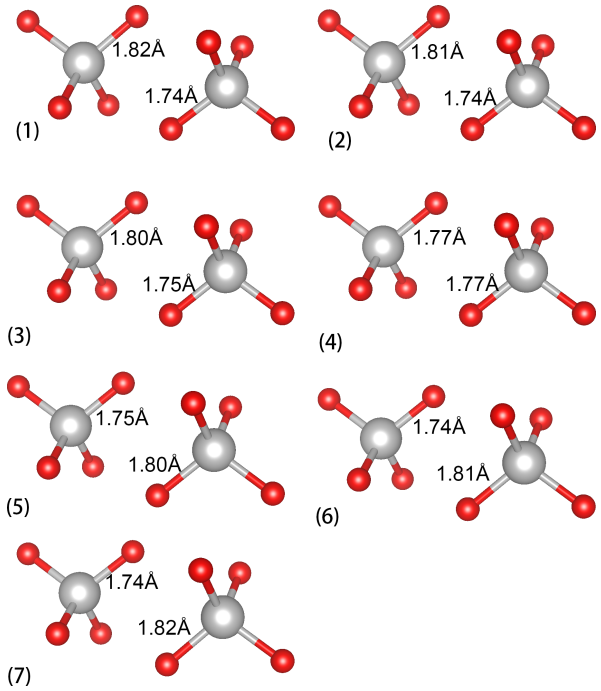

FIG. S7. Local structures of two VO_4 tetrahedra of 7 images from the CI-NEB calculation of pristine $BiVO_4$ calculation. Only 1 V-O bond length is shown in the figure, the difference of 4 V-O bond length in the same VO_4 tetrahedra is smaller than 0.01Å

* yuanping@ucsc.edu

[1] P. Giannozzi, S. Baroni, N. Bonini, M. Calandra, R. Car, C. Cavazzoni, D. Ceresoli, G. L. Chiarotti, M. Cococcioni, I. Dabo, A. Dal Corso, S. de Gironcoli, S. Fabris, G. Fratesi, R. Gebauer, U. Gerstmann, C. Gougoussis, A. Kokalj, M. Lazzeri, L. Martin-Samos, N. Marzari, F. Mauri, R. Mazzarello, S. Paolini, A. Pasquarello, L. Paulatto, C. Sbraccia, S. Scandolo, G. Sclauzero, A. P. Seitsonen, A. Smogunov, P. Umari, and R. M. Wentzcovitch, J. Phys.: Condens. Matter **21**, 395502 (2009).

[2] P. Giannozzi, O. Andreussi, T. Brumme, O. Bunau, M. B. Nardelli, M. Calandra, R. Car, C. Cavazzoni, D. Ceresoli, M. Cococcioni, N. Colonna, I. Carnimeo, A. D. Corso, S. de Gironcoli, P. Delugas, R. A. D. Jr, A. Ferretti, A. Floris, G. Fratesi, G. Fugallo, R. Gebauer, U. Gerstmann, F. Giustino, T. Gorni, J. Jia, M. Kawamura, H.-Y. Ko, A. Kokalj, E. Kkbenli, M. Lazzeri, M. Marsili, N. Marzari, F. Mauri, N. L. Nguyen, H.-V. Nguyen, A. O. de-la Roza, L. Paulatto, S. Ponc, D. Rocca, R. Sabatini, B. Santra, M. Schlipf, A. P. Seitsonen, A. Smogunov, I. Timrov, T. Thonhauser, P. Umari, N. Vast, X. Wu, and S. Baroni, J. Phys.: Condens. Matter **29**, 465901 (2017).

[3] J. P. Perdew, K. Burke, and M. Ernzerhof, Phys. Rev. Lett. **77**, 3865 (1996).

[4] J. P. Perdew, K. Burke, and M. Ernzerhof, Phys. Rev. Lett. **78**, 1396 (1997).

[5] H. S. Park, K. E. Kweon, H. Ye, E. Paek, G. S. Hwang, and A. J. Bard, J. Phys. Chem. C **115**, 17870 (2011).

[6] I. V. Solovyev, P. H. Dederichs, and V. I. Anisimov, Phys. Rev. B **50**, 16861 (1994).

[7] K. F. Garrity, J. W. Bennett, K. M. Rabe, and D. Vanderbilt, Comput. Mater. Sci. **81**, 446 (2014).

[8] D. R. Hamann, Phys. Rev. B **88**, 085117 (2013).

[9] M. Schlipf and F. Gygi, Comput. Phys. Commun. **196**, 36 (2015).

[10] M. B. Goldey, N. P. Brawand, M. Vrs, and G. Galli, J. Chem. Theory Comput. **13**, 2581 (2017).

[11] G. Kresse and J. Hafner, Phys. Rev. B **47**, 558 (1993).

[12] G. Kresse and J. Hafner, Phys. Rev. B **49**, 14251 (1994).

[13] G. Kresse and J. Furthmller, Comput. Mater. Sci. **6**, 15 (1996).

[14] G. Kresse and J. Furthmüller, Phys. Rev. B **54**, 11169 (1996).

[15] P. E. Blöchl, Phys. Rev. B **50**, 17953 (1994).

[16] G. Kresse and D. Joubert, Phys. Rev. B **59**, 1758 (1999).

[17] A. Togo and I. Tanaka, Scr. Mater. **108**, 1 (2015).

[18] G. Henkelman, B. P. Uberuaga, and H. Jnsson, J. Chem. Phys. **113**, 9901 (2000).

[19] G. Henkelman and H. Jnsson, J. Chem. Phys. **113**, 9978 (2000).

[20] G. Henkelman and H. Jnsson, J. Chem. Phys. **111**, 7010 (1999).

[21] P. Xiao, D. Sheppard, J. Rogal, and G. Henkelman, J. Chem. Phys. **140**, 174104 (2014).

[22] D. Frenkel and B. Smit, *Understanding Molecular Simulation: From Algorithms to Applications*, Computational science series (Elsevier Science, 2001).